





Seismic performance evaluation of base-isolated buildings with variations of mass and stiffness

 Zeliha Tonyali^a and  Adnan Kiral^{a*}

^a*Recep Tayyip Erdogan University, The Faculty of Engineering and Architecture, Department of Civil Engineering, Rize, 53100, Turkey*

ARTICLE INFO

Article history:

Received 23 December 2024

Received in revised form 2 March 2025

Accepted 27 March 2025

Available online

Keywords:

Base isolation

MATLAB modelling

Mass and stiffness change

Dynamic analysis

LRB

ABSTRACT

Significant investigations have been undertaken regarding base-isolated structures. However, various factors, such as substantial renovations in base-isolated buildings, the installation of heavy machinery in base-isolated hospitals, or the degradation of isolator stiffness, can lead to changes in a building's mass and stiffness over time. These alterations, often overlooked in existing literature, can affect the structure's natural period, resulting in seismic accelerations and bearing displacements that may exceed anticipated limits. This issue has not been thoroughly explored in the base isolation literature. Consequently, this study examines a nine-story isolated building whose seismic performance has been experimentally validated. The building is modelled using MATLAB platform, which is also verified by experimental findings. The results indicate that variations in mass and stiffness in base-isolated buildings can result in increased isolator bearing displacement and overall frame acceleration. Consequently, this concern highlights the need for additional vibration control measures for base-isolated buildings to prevent excessive acceleration and bearing damage.

I. INTRODUCTION

Earthquakes are a natural disaster that cannot be avoided, occurring regularly across the globe. Although prevention is not feasible, it is possible to design buildings that mitigate their negative impacts on residents and the environment [1-7]. Studies have shown that the primary cause of fatalities during earthquakes is often the collapse of buildings rather than the seismic events themselves. Despite considerable progress in earthquake engineering towards the end of the last century, catastrophic failures of structures continue to be reported in areas experiencing intense ground motion earthquakes [8-12]. Various elements, such as substandard materials, inadequate design, adverse soil conditions, and outdated construction methods, contribute to the susceptibility of buildings to earthquakes. It is crucial to mitigate potential earthquake damage, which can result in numerous injuries, fatalities, and significant structural harm. By addressing these weaknesses, the risk of earthquake-related damage can be substantially reduced, thereby preserving lives through enhanced design, superior construction practices, and retrofitting measures [13-19]. Investing in earthquake-resistant infrastructure enables the creation of buildings that are more capable of withstanding the challenges posed by natural disasters. Critical facilities, including hospitals and major government buildings, must remain fully functional immediately following an earthquake. Consequently, these structures must be engineered to endure severe seismic events to safeguard human lives, minimize economic losses, ensure the continuity of essential services, and bolster community resilience. Over recent decades, numerous researchers have explored innovative structural protection strategies aimed at

*Corresponding author. Tel.: +90-464-223-7518; e-mail: adnan.kiral@erdogan.edu.tr

enhancing a building's capacity to dissipate energy or reduce seismic damage [20-23]. Implementing energy dissipation mechanisms within buildings is essential for mitigating the effects of seismic forces and enhancing structural resilience to earthquakes [24-29].

The configuration of Lead Rubber Bearings (LRB) is crucial for ensuring effective protection against seismic events. A key attribute of LRB is its elevated vertical stiffness, which allows for lateral displacement with reduced horizontal stiffness, enabling it to support substantial vertical loads [30-32]. The adaptability of LRB is significant, as it can alter a structure's natural period, thus mitigating the potential for resonance [33]. Research indicates that isolators can endure acceptable deformation levels when exposed to far-field (FF) ground motions; however, their displacements markedly increase under near-field (NF) ground excitations [34]. This scenario can lead to heightened overall construction costs, as larger isolators may be required for buildings situated in NF zones, which contradicts the fundamental purpose of employing seismic isolators. Additionally, certain characteristics, such as peak velocity and pulse duration, in LRB-isolated structures may lead to inadequate performance and instability within the isolation system. Given that the LRB system is a widely utilized isolation technique encompassing all essential features of base isolation, it is critical to examine the factors that affect the dynamic behaviour of an isolated system [35]. Research indicates that traditional design methodologies often fail to consider the variability inherent in lead core performance and rubber properties, leading to erroneous predictions regarding the behaviour of isolators during seismic events. Under conditions of high shear strain, the elastomer demonstrates a stiffening response attributed to rubber crystallization. Additionally, cyclic loading at moderate to high shear strains typically results in a notable degradation of strength, a phenomenon that has been empirically observed. Two significant manifestations of this degradation are the Mullins effect and scragging [36]. The Mullins effect pertains to the transient damage that accumulates during the cycling of rubber, while scragging refers to the permanent damage sustained by the rubber at peak strain levels [37].

Significant deformation of LRBs is particularly evident in regions with high seismic intensity or near fault lines. Critical infrastructures, such as nuclear power facilities and hospitals, necessitate precise modelling of LRBs to effectively predict seismic demands and the characteristics of isolation layers. These structures are essential and are generally constructed with enhanced seismic safety margins, often approaching their ultimate strain capacity [38, 39]. Research conducted by Chen et al. [40] emphasizes the critical role of integrating material degradation considerations into the design of LRB isolators. Their analysis indicates that models that account for stiffness loss yield more precise insights into the performance of LRBs under cyclic loads. They introduce a generalized Bouc-Wen model, which adeptly simulates the complex nonlinear responses of LRBs during seismic events. This model is distinguished by its capacity to accurately reflect the properties of large strain stiffening and strength degradation in rubber, offering improvements over traditional modelling approaches. A further study of the influence of seawater erosion and ageing on LRBs in the context of offshore bridges was conducted by Li et al. [41].

The findings indicated that the stiffness of LRBs escalated with both ageing and prolonged exposure to seawater erosion, leading to significant alterations in the material properties of the rubber. This degradation of LRBs notably influenced the seismic resilience of offshore bridge infrastructures. Numerous studies [42, 43] have explored the role of LRBs within isolation systems, particularly concerning variations in building mass. The outcomes of these investigations reveal that fluctuations in building mass can considerably affect critical parameters such as base shear and inter-story drift, thereby affecting the seismic behaviour of structures utilizing LRBs. As determined by

Özer [44], variations in the stiffness of the rubber-bearing isolator and the mass of a building affect the structural response to seismic activity. Shin and Lee [45] investigated the effects of mass eccentricity on base-isolated structures, with a particular focus on nuclear power plants, revealing that even minor variations in mass can impact seismic performance. Their research highlighted the importance of mass distribution within the superstructure for preserving the intended isolation characteristics. By incorporating these considerations into design frameworks, structural engineers can enhance the geometric and mechanical properties of LRBs, thereby effectively addressing potential failure modes such as rubber rupture, strength degradation, and changes in building mass. As a result, structures equipped with a base isolation (BI) system may undergo considerable alterations in their mass and lateral resistance over time, which can subsequently affect their natural frequencies and seismic responses in terms of LRB drift and floor acceleration.

In pursuit of deeper insights into the modification of building mass and bearing stiffness, this study performs numerical analysis on a Multi-Degree-of-Freedom (MDOF) isolated building that has been verified through experimental study. The modelling of the building is executed within the MATLAB environment [46]. The findings of this research may illuminate the implications of changes in mass alone, LRB stiffness alone, or the combination of both factors.

II. NUMERICAL STUDY

2.1 Building properties

Sosokan, a building at Keio University, was completed in the year 2000 and is equipped with a base isolation system at its foundational level. The construction utilizes steel-reinforced concrete, concrete-filled steel tubes, and steel components. It features a total of nine floors, which include one basement and eight stories above ground. The isolation layer comprises 65 laminated LRBs. Kohiyama et al. [47] calculated the building's parameters, such as damping coefficient, stiffness and mass, by compiling experimental data from several past seismic events. In Table 1, these values are outlined, where B2F, B1F, 1F, and RF denote the second basement, the first basement, the first floor, and the roof floors, respectively. The isolation layer is denoted B2F in Table 1. In Section 2.1, the total mass, damping coefficient and stiffness of the LRB are indicated as m_1 , c_1 and k_1 , respectively. For further insights into the building model adopted in this study, see the reference by Kiral and Gurbuz [21].

Table 1. Structural parameters of the building [47]

Floor	Mass (10^6 kg)	Stiffness (10^9 N/m)	Damping (10^6 Ns/m)
RF	2.500	0.962	6.225
7 F	2.066	1.203	7.777
6 F	2.037	1.478	9.555
5 F	2.037	1.807	11.687
4F	2.050	2.154	13.930
3F	2.033	1.975	12.773
2F	1.826	2.138	13.827
1F	2.491	2.930	18.946
B1F	3.439	2.232	14.437
B2F	4.981	0.104	0.000

2.2. Mathematical representation and design of the adopted building

The equation that presents the motion of the building system is stated by Dan and Kohiyama [48] as follows:

$$M \ddot{x} + C \dot{x} + K x = F \ddot{z} \quad (1)$$

with

$$x = [x_1 \ x_2 \ \cdots \ x_{10}]^T \quad (2a)$$

$$M = \text{diag}(m_1, m_2, \cdots, m_{10}) \quad (2b)$$

$$C = \begin{bmatrix} c_1 + c_2 & -c_2 & \cdots & 0 & 0 \\ -c_2 & c_2 + c_3 & & & 0 \\ \vdots & & \ddots & & \vdots \\ 0 & & & c_9 + c_{10} & -c_{10} \\ 0 & 0 & \cdots & -c_{10} & +c_{10} \end{bmatrix} \quad (2c)$$

$$K = \begin{bmatrix} k_1 + k_2 & -k_2 & \cdots & 0 & 0 \\ -k_2 & k_2 + k_3 & & & 0 \\ \vdots & & \ddots & & \vdots \\ 0 & & & k_9 + k_{10} & -k_{10} \\ 0 & 0 & \cdots & -k_{10} & +k_{10} \end{bmatrix} \quad (2d)$$

$$F = [-m_1 \ -m_2 \ \cdots \ -m_{10}]^T \quad (2e)$$

where M, C and K are mass, damping and stiffness matrices, respectively. x is the displacement vector. \ddot{z} is ground acceleration. Eq. (3) illustrates the state space that corresponds to Eq. (1).

$$\dot{x}_t = A x_t + D \ddot{z} \quad (3)$$

where

$$x_t = \begin{bmatrix} x \\ \dot{x} \end{bmatrix}, \quad A = \begin{bmatrix} 0_{10 \times 10} & I_{10 \times 10} \\ -M^{-1}K & -M^{-1}C \end{bmatrix}, \quad \text{and} \quad D = \begin{bmatrix} 0_{10 \times 1} \\ M^{-1}F \end{bmatrix} \quad (4)$$

Verifying the correctness of the MATLAB code is of the utmost importance before the commencement of simulation construction. As such, the MATLAB code currently in use has been validated with experimental data,

as previously discussed in the work of Kiral and Gurbuz [21]. The modelling process for the Sosokan building in MATLAB involves several critical steps. Initially, the state space representation is formulated, as described in Eqs. 3-4 of this study. MATLAB's "ss" command is employed to develop a state-space model based on the parameters detailed in Table 1. Next, earthquake data, specifically from one of the ground motion records listed in Table 2, is incorporated into the MATLAB simulation file. Finally, the "lsim" command is utilized to visualize the simulated time response of the model, with the recognition that MATLAB [46] operates using Kernels for Linear Time Invariant Systems. The building models under consideration are outlined as follows:

Sys_{ini} : This model represents the initial design, which includes previously calculated total mass and LRB stiffness for the building. The first period (T_1) is 3.1s.

$Sys_{red,m}$: This model presents reduced mass, where the building's overall mass is decreased by 10%. The first period of this model is 2.98s.

$Sys_{inc,m}$: In this scenario, the mass of the building is increased by 10%. The first period of this model is 3.3s.

$Sys_{red,LRB}$: In this scenario, the total stiffness of the LRB is reduced by 10%. The first period of this model is 3.12s.

$Sys_{redLRB\&incM}$: In this scenario, the total stiffness of the LRB is reduced by 10% and the total mass of the building is increased by 10%. The first period of this model is 3.3s.

2.3. Seismic records

Kohiyama et al. [47] conducted research on the Sosokan building by synthesizing 1,000 simulated ground motions classified as "rare earthquake motion" and "very rare earthquake motion," in accordance with Notification No. 1461 from the Ministry of Construction, Japan, dated May 31, 2000. To create waves with varying ground motion intensities, they linearly interpolated the parameters for wave amplitude envelope curves and designed response spectra between the two specified earthquake types. The simulations were designed to last between 60 and 120 seconds, with peak ground velocities (PGV) ranging from 0.0821 to 0.5643 meters per second. The analysis presented in this study included one specific generated record (simulation number = 600; for more details, see the ref. Kohiyama et al. [47]) alongside natural ground motion, as shown in Table 2 and Figure 1. It is important to mention that this study is limited to these two earthquake records. More earthquake records could be needed for deeper evaluations.

Table 2. Selected ground motion records [21, 47]

Earthquake	Mw	Abbreviation	Station ID/component	PGA (m/s^2)
2011 Tohoku	9.1	Tohoku	Tohoku/EW	0.711
Generated	6.9	SIM	-	2.510

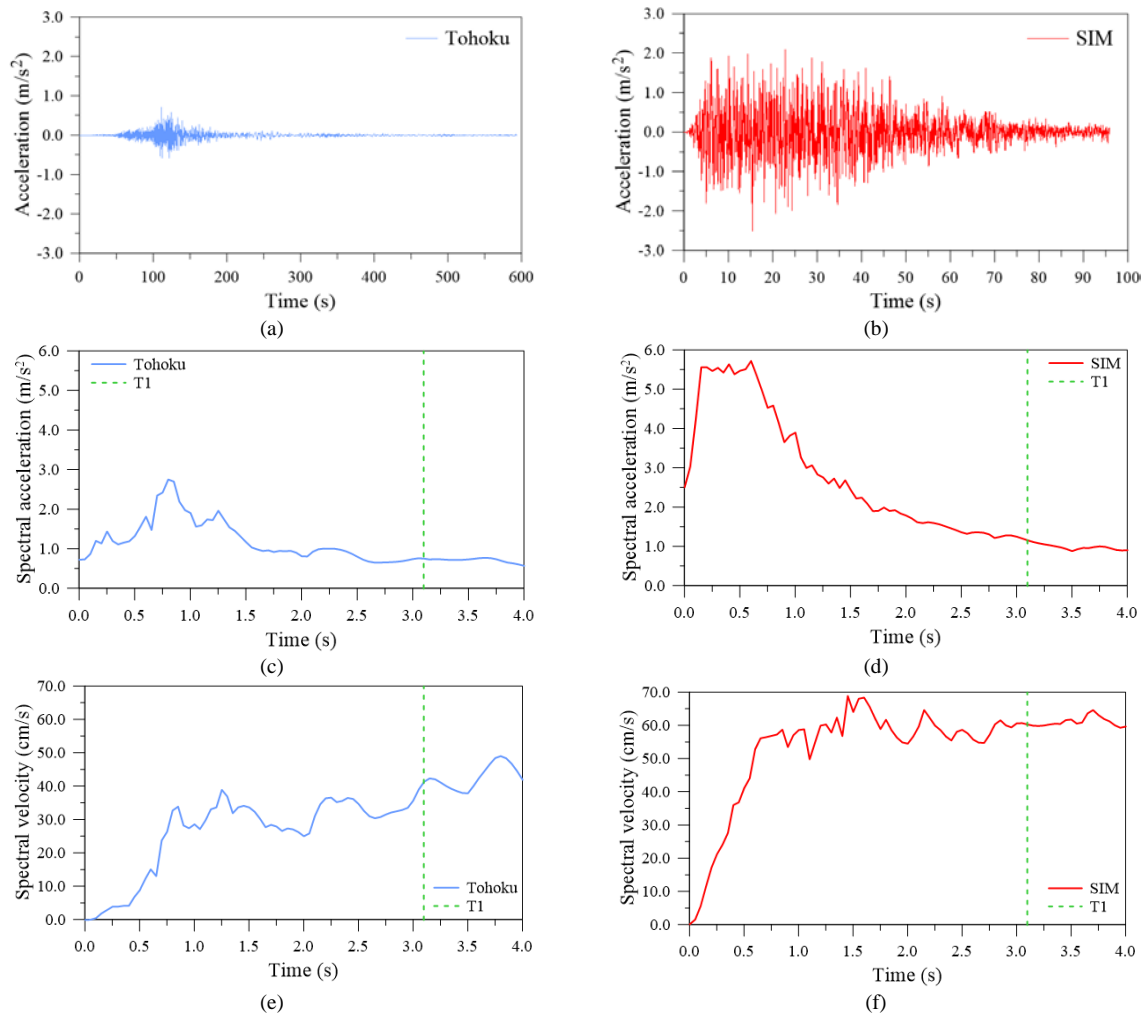


Figure 1. Input accelerations, spectral accelerations, and spectral velocities of two earthquakes

III. RESULTS AND DISCUSSIONS

3.1. System modification in only mass

Figure 2 and Table 3 illustrates the seismic response of the three models during the Tohoku earthquake. In this section and the subsequent ones, the results of Sys_{ini} , such as displacement and acceleration, will serve as a reference for clarity. When the total mass of Sys_{ini} is decreased by 10%, the LRB displacement and the absolute acceleration of the RF increase by 36% and 56%, respectively, during the Tohoku earthquake. This modified model is referred to $Sys_{red,m}$ (see Figure 2a2-b2). Conversely, when the total mass of Sys_{ini} is increased by 10%, the results indicate that LRB displacement and RF acceleration rise by 44% and 27%, respectively, under the same seismic event (see Figure 2a3- b3). The evaluation of the three model is also executed under SIM earthquake, as illustrated in Figure 3 and detailed in Table 3. As mentioned before, this analysis relies on the findings from Sys_{ini} , particularly focusing on displacement and acceleration as a comparative baseline with other models. A 10% decrease in the total mass of Sys_{ini} results in a 22% increase in LRB displacement and a 55% increase in the absolute acceleration of the RF, with this revised model designated $Sys_{red,m}$ (see Figure 3a2-b2). In contrast, an increase of 10% in the total mass of Sys_{ini} results in a 42% increase in LRB displacement and a 30% increase in RF acceleration (named $Sys_{inc,m}$; see Figure 3a3-b3). It is crucial to note that in both $Sys_{red,m}$ and $Sys_{inc,m}$, RF

acceleration and LRB displacement are found to increase during both earthquakes. This phenomenon is attributed to the rise in spectral acceleration values for $Sys_{red,m}$ and the increase in mass for $Sys_{inc,m}$ (see Figure 1c and d).

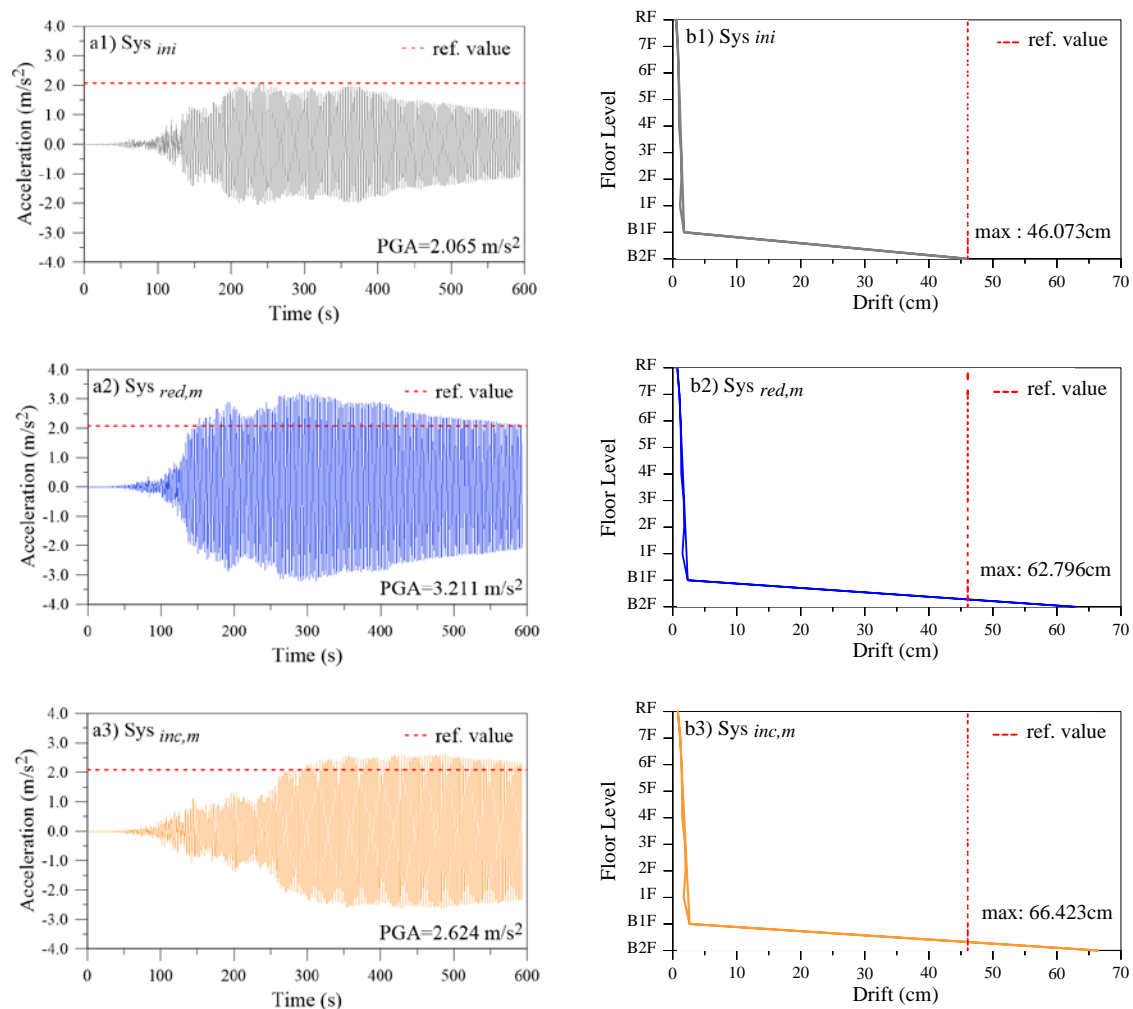


Figure 2. (a1-a3) The acceleration-time history and (b1-b3) floor drifts of the systems in the case of Sys_{ini} , $Sys_{red,m}$ and $Sys_{inc,m}$ under Tohoku earthquake, respectively.

Table 3. Main results of models subjected to Tohoku and SIM earthquakes (Δ =reduction)

Record	Systems	Max. LRB disp. (cm)	Δ	Max. acceleration of RF (m/s^2)	Δ
Tohoku	Sys_{ini}	46.07	-	2.06	-
	$Sys_{red,m}$	62.80	+36%	3.21	+56%
	$Sys_{inc,m}$	66.42	+44%	2.62	+27%
SIM	Sys_{ini}	31.56	-	1.59	-
	$Sys_{red,m}$	38.48	+22%	2.47	+55%
	$Sys_{inc,m}$	44.89	+42%	2.06	+30%

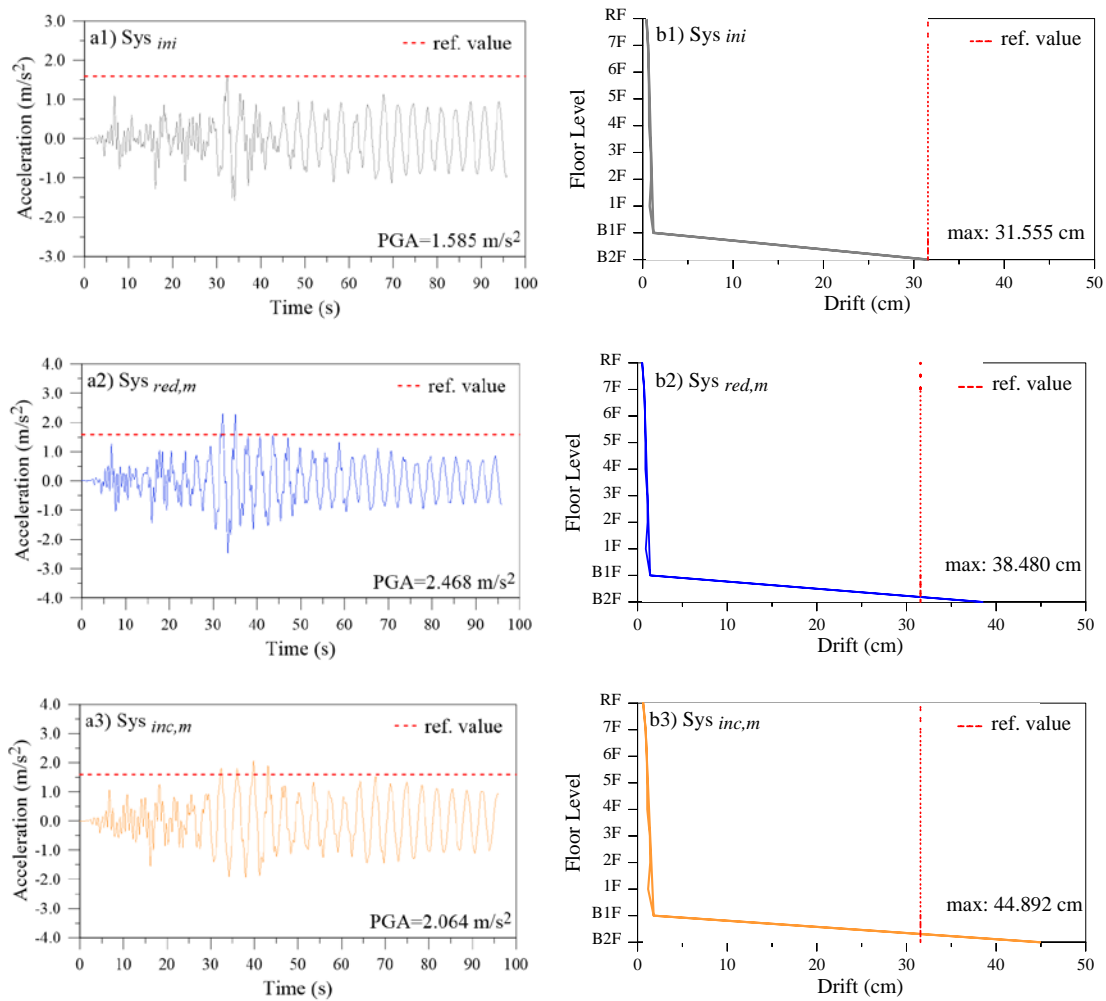


Figure 3. (a1-a3) The acceleration-time history and (b1-b3) floor drifts of the systems in the case of Sys_{ini} , $Sys_{red,m}$ and $Sys_{inc,m}$ under SIM excitation, respectively.

3.2. System modification in only LRB stiffness

The seismic responses of the two models during the Tohoku earthquake are depicted in Figure 4 and detailed in Table 4. A 10% reduction in the total LRB stiffness of Sys_{ini} (see Figure 4a1-b1) leads to a 12% increase in LRB displacement and a 10% increase in the absolute acceleration of the RF. This new model is named $Sys_{red,LRB}$ (see Figure 4a2-b2). The evaluation of the two model are further examined under SIM earthquakes, as shown in Figure 5 and described in Table 4. This analysis, as previously indicated, is based on the findings from Sys_{ini} , with a particular focus on displacement and acceleration for comparative purposes with the other models (see Figure 5 a1-b1). A reduction of 10% in the overall LRB stiffness of Sys_{ini} leads to a 26% increase in LRB displacement and a 19% increase in the absolute acceleration of the RF, with this modified model referred to $Sys_{red,LRB}$ (see Figure 5a2-b2). It is necessary to note that in the analysis of $Sys_{red,LRB}$, both LRB displacement and RF acceleration increase when subjected to two earthquake records. This outcome is anticipated, as a decrease in the stiffness of the LRB will lead to greater displacement. Furthermore, the changes in spectral velocity values that occur with alterations in period also contribute to the increased acceleration observed under both earthquakes (refer to Figure 1e and f).

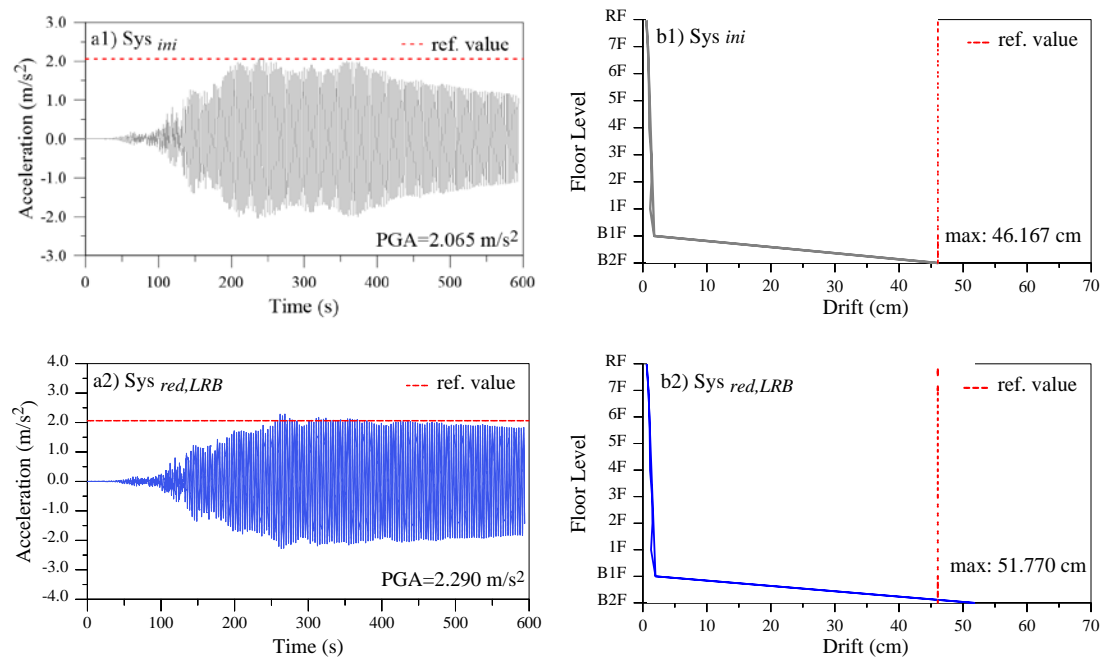


Figure 4. (a1-a2) The acceleration-time history and (b1-b2) floor drifts of the systems in the case of Sys_{ini} and $Sys_{red,LRB}$ under Tohoku earthquake, respectively.

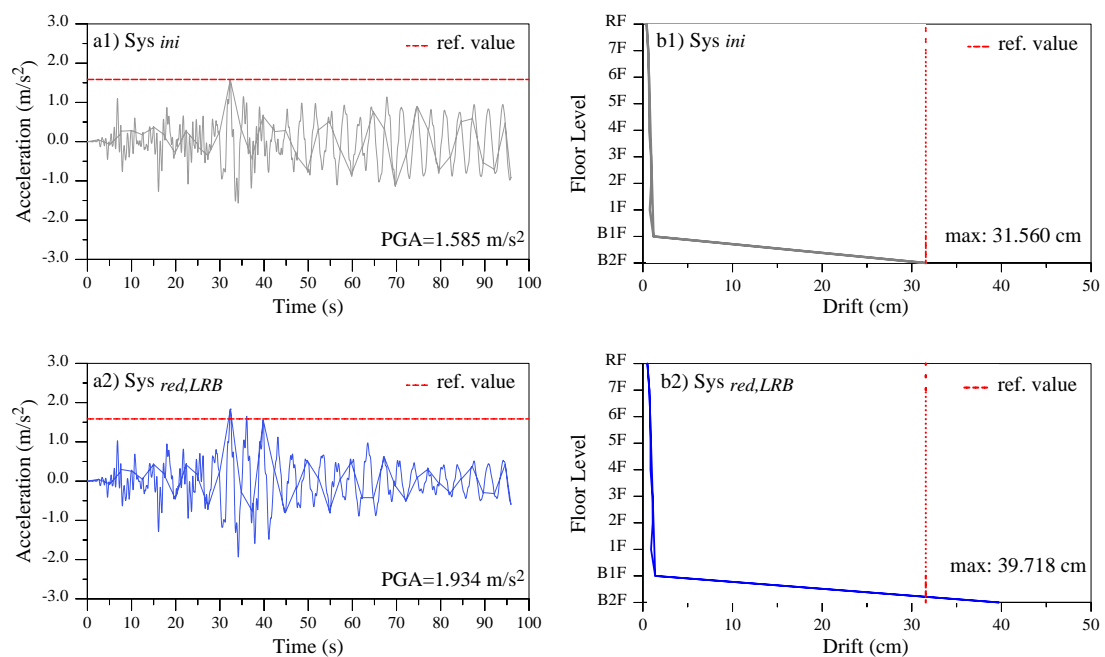


Figure 5. (a1-a2) The acceleration-time history and (b1-b2) floor drifts of the systems in the case of Sys_{ini} and $Sys_{red,LRB}$ under SIM excitation, respectively.

Table 4. Main results of models subjected to Tohoku and SIM earthquakes (Δ =reduction)

Record	Systems	Max. LRB disp. (cm)	Δ	Max. acceleration of RF (m/s ²)	Δ
Tohoku	Sys_{ini}	46.1	-	2.1	-
	$Sys_{red,LRB}$	51.8	+12%	2.3	+10%
SIM	Sys_{ini}	31.6	-	1.6	-
	$Sys_{red,LRB}$	39.7	+26%	1.9	+19%

3.3. System modification in both building's mass and LRB stiffness

Figure 6 shows the two models' seismic responses during the Tohoku earthquake, while Table 5 provides the main results. A 10% increase in Sys_{ini} mass and a 10% decrease in overall LRB stiffness result in a 26% increase in the RF's absolute acceleration and a 42% increase in LRB displacement. $Sys_{redLRB\&incM}$ is the new model's name. Under SIM earthquakes, the two model are further evaluated and discussed in Table 5 and Figure 7. As previously mentioned, the results from Sys_{ini} serve as the basis for this study, which focuses in particular on displacement and acceleration for comparison with the other models. $Sys_{redLRB\&incM}$ results in a 121% increase in LRB displacement and a 67% increase in the absolute acceleration of the RF following a 10% reduction in total LRB stiffness and a 10% increase in Sys_{ini} 's mass. It is important to highlight that the findings from $Sys_{redLRB\&incM}$ indicate an increase in both the displacement of the LRB and the RF acceleration when exposed to two distinct earthquake records. This occurrence can be explained by an increase in the model's overall mass, which leads to a rise in acceleration, coupled with a reduction in the stiffness of the LRB, resulting in greater displacement of the LRB.

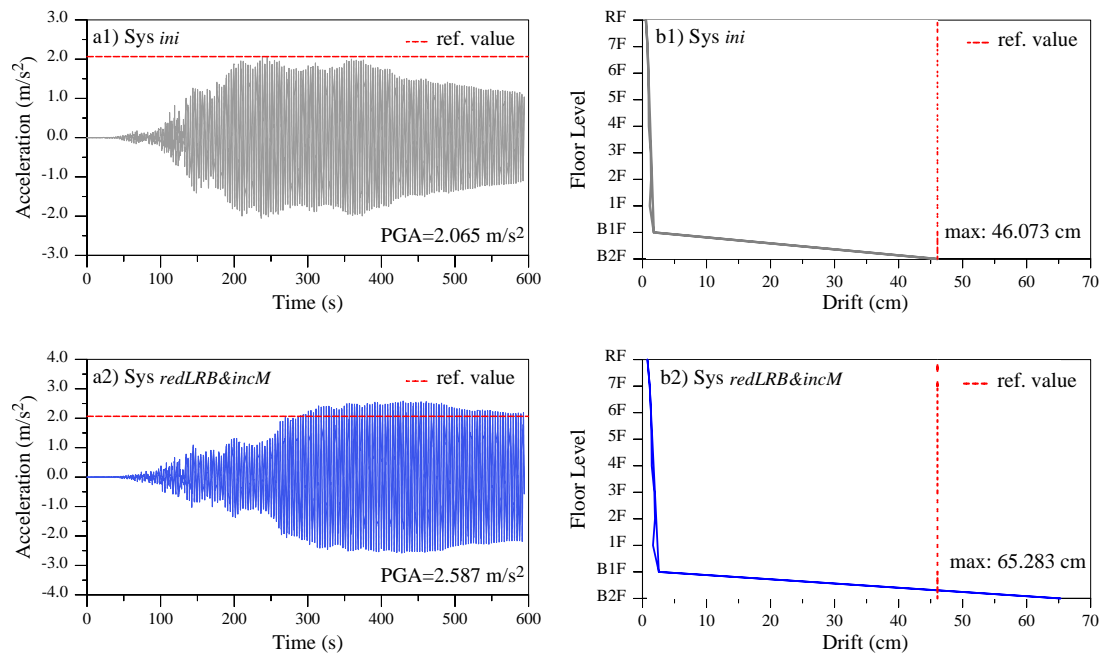


Figure 6. (a1-a2) The acceleration-time history and (b1-b2) floor drifts in the case of Sys_{ini} and $Sys_{redLRB\&incM}$, under Tohoku earthquake, respectively.

Table 5. Main results of models subjected to Tohoku and SIM earthquakes (Δ =reduction)

Record	Systems	Max. LRB disp. (cm)	Δ	Max. acceleration of RF (m/s^2)	Δ
Tohoku	Sys_{ini}	46.07	-	2.06	-
	$Sys_{redLRB\&incM}$	65.28	+42%	2.59	+26%
SIM	Sys_{ini}	31.55	-	1.59	-
	$Sys_{redLRB\&incM}$	69.64	+121%	2.66	+67%

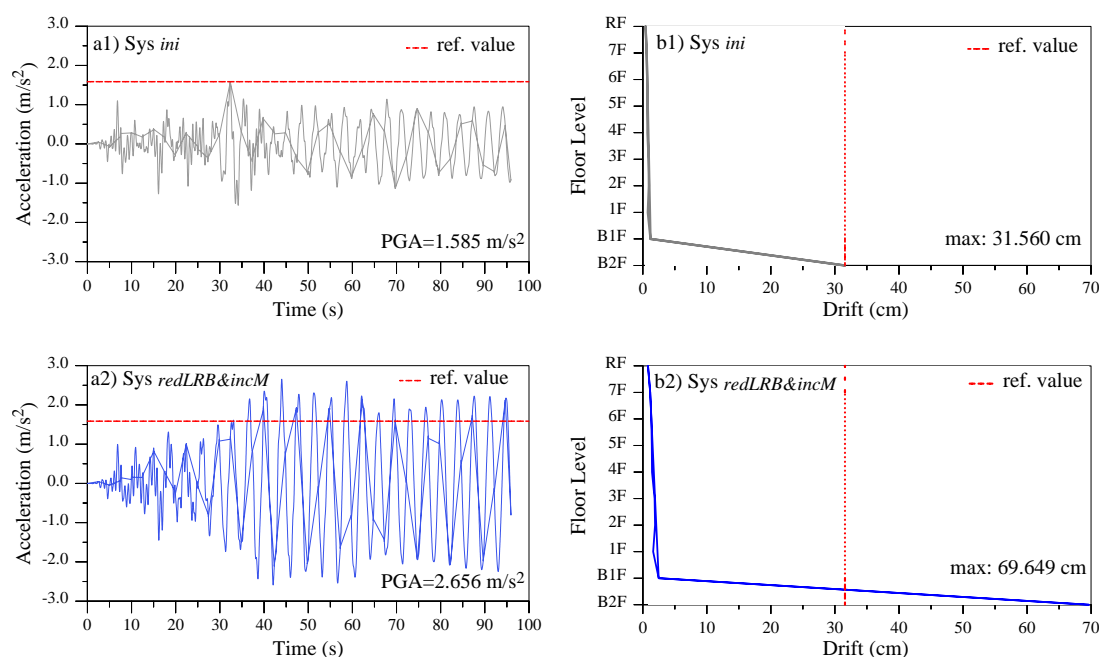


Figure 7. (a1-a2) The acceleration-time history and (b1-b2) floor drifts in the case of Sys_{ini} and $Sys_{redLRB\&incM}$ under SIM earthquake, respectively.

IV. CONCLUSIONS

In this study, responses from Sys_{ini} , $Sys_{red,m}$, $Sys_{inc,m}$, $Sys_{red,LRB}$ and $Sys_{redLRB\&incM}$ models under one simulated and one observed earthquake are analytically evaluated. This research takes into consideration the nine-story building called "Sosokan," which is situated at Keio University in Japan. According to the experimental findings of Kohiyama et al. [47], the chosen building model in MATLAB is validated in this study. The purpose of this research is to investigate the acceleration and displacement responses of different building models to seismic activity. It is important to mention that this study is limited to linear dynamic analysis by assuming that all structural element (beams, columns, slabs and LRBs) remains in linear region of their capacity. Also, it is assumed that the vertical load capacity of LRBs is also sufficient under these three building model scenarios. It is important to acknowledge that the ratios obtained are valid solely for the selected earthquake records and the MATLAB model utilized in this analysis. The following findings were drawn from the study's analysis:

- In the building's overall mass is decreased by 10% ($Sys_{red,m}$) the maximum LRB displacement and the RF acceleration increased up to 36% and 56%, respectively, under two earthquakes. Similarly, in the building's overall mass is decreased by 10% ($Sys_{inc,m}$) the maximum LRB displacement and the RF acceleration increased up to 44% and 30%, respectively.
- In the reducing LRB stiffness is decreased by 10% ($Sys_{red,LRB}$), the maximum LRB displacement and the RF acceleration increased up to 26% and 19%, respectively, under two earthquakes.
- The maximum LRB displacement and the RF acceleration increased up to 121% and 67%, respectively, for reduced LRB stiffness and increasing building' mass models ($Sys_{redLRB\&incM}$) under two earthquakes.

The findings of this research indicate that future investigations should explore various vibration control strategies within the base isolation layer to mitigate potential damage to isolation bearings and to address undesirable accelerations resulting from changes in mass and LRB stiffness. One possible alternative could be the implementation of viscous dampers at the base, which could effectively reduce both acceleration and LRB drift. A future study will consider such damper and propose novel design methodologies for damping coefficient selection.

ACKNOWLEDGEMENTS

The authors would like to thank anonymous reviewers for their feedback.

REFERENCES

1. Kiral A, Ergün M, Tonyali Z, Artar M, Şentürk İ (2024) A case study comparing seismic retrofitting techniques for a historically significant masonry building's minaret. *Engineering Failure Analysis*, 166, 108873. <https://doi.org/10.1016/j.engfailanal.2024.108873>
2. Zhao Y, Huang P, Long G, Yuan Y, and Sun Y (2020) Influence of fluid viscous damper on the dynamic response of suspension bridge under random traffic load. *Advances in Civil Engineering*, 1, 1857378. <https://doi.org/10.1155/2020/1857378>
3. Lin J (2022) Vibration reduction performance of structures with viscous dampers under near-field earthquakes. *Advances in Civil Engineering*, 2022, 1, 1315213. <https://doi.org/10.1155/2022/1315213>
4. Wei L, Nie H (2022) Seismic vulnerability analysis of prefabricated concrete frame with a cam-type response amplifying device of viscous damper. *Advances in Civil Engineering*, 2022, 1, 3386719. <https://doi.org/10.1155/2022/3386719>
5. Q. Zhang, Z.-y. Wei, J.-x. Gong, P. Yu, and Y.-q. Zhang (2018) Equivalent viscous damping ratio model for flexure critical reinforced concrete columns. *Advances in Civil Engineering*, 2018, 1, 5897620. <https://doi.org/10.1155/2018/5897620>
6. Günaydın M, Tonyali Z (2018) Dynamic response of a reinforced concrete minaret. *J. Struct. Eng. Appl. Mech*, 1: 2, 62-72.
7. Kiral A, Tonyali Z, Ergün M (2025) A comprehensive analysis of the ground motions of the 2023 Kahramanmaraş, Türkiye earthquakes. *Earthquake and Structures*, 26, 203-219, <https://doi.org/10.12989/eas.2025.28.3.203>
8. Idham NC (2018) Earthquake failures on buildings and the role of architect on building safety. *Dimensi: Journal of Architecture and Built Environment*, 45: 2, 153-164. <https://doi.org/10.9744/dimensi.45.2.153-164>
9. Tonyali Z, Kiral A (2024) Evaluation of Earthquake-Related Damages on the Reinforced Concrete Buildings due to the February 6, 2023, Kahramanmaraş-Türkiye Earthquakes. *Recep Tayyip Erdogan University Journal of Science and Engineering*, 5:1, 89-114. <https://doi.org/10.53501/rteufemud.1471964>
10. Ivanov ML, Chow WK (2023) Structural damage observed in reinforced concrete buildings in Adiyaman during the 2023 Türkiye Kahramanmaraş Earthquakes. *Structures*, 58, 105578. <https://doi.org/10.1016/j.istruc.2023.105578>
11. Li N, Zhu B, Zhang L, Kishiki S (2024) Damage analysis of a pseudoclassic reinforced concrete frame structure under the action of the Ms 6.8 Luding earthquake in China. *Structures*, 60, 105887. <https://doi.org/10.1016/j.istruc.2024.105887>
12. Tonyali Z, Yurdakul M, Sesli H (2022) Dynamic response of concentrically braced steel frames to pulse period in near-fault ground motions," *Turkish Journal of Science and Technology*, 17: 2, 357-373. <https://doi.org/10.55525/tjst.1113021>
13. Chopra AK (1995) Theory and applications to earthquake engineering, *Dyn Struct*, 1995.
14. Aydogdu HH, Demir C, Kahraman T, Ilki A (2023) Evaluation of rapid seismic safety assessment methods on a substandard reinforced concrete building stock in Istanbul. *Structures*, 56, 104962. <https://doi.org/10.1016/j.istruc.2023.104962>
15. Stepinac M, Bedon C, Funari MF, Kišiček T, Hancilar U (2024) Assessment, Reconstruction and Decision Procedures for the Preservation of Existing Structures after Earthquakes," ed: MDPI-Multidisciplinary Digital Publishing Institute.

16. Impollonia N, Palmeri A (2018) Seismic performance of buildings retrofitted with nonlinear viscous dampers and adjacent reaction towers. *Earthquake Engineering & Structural Dynamics*, 47: 5, 1329-1351. <https://doi.org/10.1002/eqe.3020>
17. Palmeri A (2006) Correlation coefficients for structures with viscoelastic dampers. *Engineering Structures*, 28: 8, 1197-1208. <https://doi.org/10.1016/j.engstruct.2005.12.015>
18. Ates S, Kahya V, Yurdakul M, Adanur S (2013) Damages on reinforced concrete buildings due to consecutive earthquakes in Van. *Soil Dynamics and Earthquake Engineering*, 53, 109-118. <https://doi.org/10.1016/j.soildyn.2013.06.006>
19. Altunışık AC, Arslan ME, Kahya V, Aslan B, Sezdirmez T, Dok G, Kirtel O, Öztürk H, Sunca F, Baltacı A, "Field observations and damage evaluation in reinforced concrete buildings after the February 6th, 2023, Kahramanmaraş–Türkiye Earthquakes," *Journal of Earthquake and Tsunami*, 17: 06, 2350024. <https://doi.org/10.1142/S1793431123500240>
20. Wong KK (2008) Seismic energy dissipation of inelastic structures with tuned mass dampers. *Journal of engineering mechanics*, 134: 2, 163-172. [https://doi.org/10.1061/\(ASCE\)0733-9399\(2008\)134:2\(163](https://doi.org/10.1061/(ASCE)0733-9399(2008)134:2(163)
21. Kiral A, Gurbuz A (2024) Using supplemental linear viscous dampers for experimentally verified base-isolated building: Case study. *Journal of Structural Engineering & Applied Mechanics (Online)*, 7: 1. <https://doi.org/10.31462/jseam.2024.01034050>
22. Sesli H, Tonyali Z, Yurdakul M (2022) An investigation on seismically isolated buildings in near-fault region. *Journal of Innovative Engineering and Natural Science*, 2: 2, 47-65. <https://doi.org/10.29228/JIENS.63395>
23. Kiral A, Garcia R, Petkovski M, Hajirasouliha I (2024) Seismic performance assessment of steel buildings equipped with a new semi-active displacement-dependent viscous damper. *Journal of Earthquake and Tsunami*. <https://doi.org/10.1142/s1793431124500222>
24. Shang Q, Wang T, Li J (2019) Seismic fragility of flexible pipeline connections in a base isolated medical building. *Earthquake Engineering and Engineering Vibration*, 18, 903-916. <https://doi.org/10.1007/s11803-019-0542-5>
25. Almajhali KYM (2023) Review on passive energy dissipation devices and techniques of installation for high rise building structures. *Structures*, 51, 1019-1029. <https://doi.org/10.1016/j.istruc.2023.03.025>
26. Ijmulwar SS, Patro SK (2024) Seismic design of reinforced concrete buildings equipped with viscous dampers using simplified performance-based approach. *Structures*, 61, 106020. <https://doi.org/10.1016/j.istruc.2024.106020>
27. A Moslehi Tabar , Domenico DD, Dindari H (2021) Seismic rehabilitation of steel arch bridges using nonlinear viscous dampers: Application to a case study. *Practice Periodical on Structural Design and Construction*, 26, 3, 04021012, [https://doi.org/10.1061/\(ASCE\)SC.1943-5576.0000576](https://doi.org/10.1061/(ASCE)SC.1943-5576.0000576)
28. A Moslehi Tabar, Domenico DD (2020) Nonlinear response spectrum analysis of structures equipped with nonlinear power law viscous dampers. *Engineering Structures*, 219, 110857. <https://doi.org/10.1016/j.engstruct.2020.110857>
29. Kiral A, Gurbuz A, Ustabas I (2024) The seismic response evaluation of an existing multi-span reinforced concrete highway bridge in the presence of linear and nonlinear viscous dampers. *Arabian Journal for Science and Engineering*, 1-19. <https://doi.org/10.1007/s13369-024-09265-2>
30. Seo J, Hu LW (2016) Seismic response and performance evaluation of self-centering lrb isolators installed on the cbf building under NF ground motions. *Sustainability*. 8: 2, 109, 2016. <https://www.mdpi.com/2071-1050/8/2/109>
31. Kiral A, Tonyali Z. (2025) The effect of LRB stiffness changes with and without supplemental viscous dampers on seismic responses of an experimentally verified MDOF building. *Sigma J. Eng. Nat. Sci.*, 43: 1, 301-315. doi: <https://doi.org/10.14744/sigma.2024.00104>
32. Kiral A, Tonyali Z. (2024) Seismic response control of buildings using viscous-based devices," in *modern approaches to traffic safety and sound insulation: BIDGE Publications*, ch. 4, pp. 70-111.
33. Haque MN, Zisan MB, Bhuiyan AR (2013) Seismic response analysis of base isolated building: Effect of lead rubber bearing characteristics. *Malaysian Journal of Civil Engineering*, 25: 2, 154-167. <https://doi.org/10.11113/mjce.v25.15849>
34. Jangid RS, Kelly JM (2001) Base isolation for near-fault motions. *Earthquake engineering & structural dynamics*, 30: 5, 691-707. <https://doi.org/10.1002/eqe.31>
35. Providakis CP (2008) Effect of LRB isolators and supplemental viscous dampers on seismic isolated buildings under near-fault excitations. *Engineering structures*, 30: 5, 1187-1198. <https://doi.org/10.1016/j.engstruct.2007.07.020>
36. Clark PW (1996) Experimental studies of the ultimate behavior of seismically-isolated structures. PhD Thesis, University of California, Berkeley.
37. Kitayama S, Constantinou MC, (2022) Performance evaluation of seismically isolated buildings near active faults. *Earthquake Engineering & Structural Dynamics*, 51: 5, 1017-1037. <https://doi.org/10.1002/eqe.3602>

38. Whittaker AS, Sollogoub P, Kim MK (2018) Seismic isolation of nuclear power plants: Past, present and future. *Nuclear Engineering and Design*, 338, 290-299. <https://doi.org/10.1016/j.nucengdes.2018.07.025>
39. Sarebanha A, Mosqueda G, Kim MK, Kim JH (2018) Seismic response of base isolated nuclear power plants considering impact to moat walls," *Nuclear Engineering and Design*, 328, 58-72. <https://doi.org/10.1016/j.nucengdes.2017.12.021>
40. Chen P, Wang B, Zhang Z, Li T, Dai K (2023) A generalized model of lead rubber bearing considering large strain stiffening and degradation. *Engineering Structures*, 275, 115264. <https://doi.org/10.1016/j.engstruct.2022.115264>
41. Li Y, Ma Y, Zhao G, Liu R (2023) Study on the basic performance deterioration law and the application of lead rubber bearings under the alternation of aging and seawater erosion. *Buildings* 13: 2, 360. <https://doi.org/10.3390/buildings13020360>
42. Darwish AQ, Bhandari M (2022) Vibration response reduction of seismic forces using lead rubber bearing isolators in composite buildings. *Journal of Vibration Engineering & Technologies*, 10: 4, 1309-1324, <https://doi.org/10.1007/s42417-022-00447-6>
43. Hu LW, Response of seismically isolated steel frame buildings with sustainable lead-rubber bearing (LRB) isolator devices subjected to near-fault (NF) ground motions. *Sustainability*, 7: 1, 111-137. <https://www.mdpi.com/2071-1050/7/1/111>
44. E. Özer (2022) Geleneksel ve taban izolatörlü betonarme binaların sismik davranışlarının karşılaştırılması (In Turkish), Ms Thesis, Civil Engineering, Pamukkale University.
45. Shin TM, Lee BC (2023) Seismic response effect on base-isolated rigid structures by mass eccentricity in nuclear plants. *Applied Sciences*, 13: 24, 13330. <https://doi.org/10.3390/app132413330>
46. MATLAB-R, <https://it.mathworks.com/help/matlab/>. Accessed Feb 2024, 2018a.
47. Kohiyama M, Omura M, Takahashi M, Yoshida O, Nakatsuka K. (2019) Update of control parameters for semi-actively controlled base-isolated building to improve seismic performance. *Japan Architectural Review*, 2:3, 226-237. <https://doi.org/10.1002/2475-8876.12090>
48. Dan M, Kohiyama M (2013) System identification and control improvement of a semi-active-controlled base-isolated building using the records of the 2011 Great East Japan earthquake. in *In 11th International Conference on Structural Safety and Reliability, ICOSSAR*, 3841-3847.